The EMBO Journal vol.15 no.2 pp.201–210, 1996

The actin binding site of thymosin β4 mapped by mutational analysis

M.Van Troys[1], D.Dewitte, M.Goethals, M.-F.Carlier[2], J.Vandekerckhove and C.Ampe

Flanders Interuniversity Institute for Biotechnology, Department of Biochemistry, Faculty of Medicine, University of Ghent, B-9000 Ghent, Belgium and [2]Laboratory of Enzymology, CNRS, 91198 Gif-sur-Yvette, France

[1]Corresponding author

We characterized in detail the actin binding site of the small actin-sequestering protein thymosin β4 (Tβ4) using chemically synthesized full-length Tβ4 variants. The N-terminal part (residues 1–16) and a hexapeptide motif (residues 17–22) form separate structural entities. In both, we identified charged and hydrophobic residues that participate in the actin interaction using chemical cross-linking, complex formation in native gels and actin-sequestering experiments. Quantitative data on the activity of the variants and circular dichroism experiments allow to present a model in which the N-terminal part needs to adopt an α-helix for actin binding and interacts through a patch of hydrophobic residues (^{6}M-I-F^{12}) on one side of this helix. Also, electrostatic contacts between actin and lysine residues 18, in the motif, and 14, in the N-terminal α-helix, appear important for binding. The residues critical for contacting actin are conserved throughout the β-thymosin family and in addition to this we identify a similar pattern in the C-terminal headpiece of villin and dematin.

Keywords: actin binding/structure–function relation/thymosin β4 mutants/villin headpiece

Introduction

Cell locomotion requires the rapid and spatially defined turnover of actin filaments. The extent and rate of their assembly and disassembly are regulated by a variety of actin-associated proteins which intervene at different steps of the actin polymerization process. A number of actin monomer binding proteins provide the cell with a large reserve of actin monomers which can rapidly be mobilized for polymerization upon cell stimulation (Fechheimer and Zigmond, 1993). Two of these proteins are profilin and thymosin β4 (Tβ4) which are postulated to act in concert whereby profilin actively participates in actin filament assembly while Tβ4 acts solely as an actin-sequestering protein (Carlier and Pantaloni, 1994).

The β-thymosins are a family of highly conserved 5 kDa polypeptides and both *in vitro* and *in vivo* studies suggest they form the bulk of actin-sequestering capacity in the cytoplasm of non-muscle cells (Safer and Nachmias, 1994). In thrombin-stimulated platelets the increase in filamentous actin (F-actin) is paralleled with a decrease in β-thymosin–actin complex (Nachmias *et al.*, 1993). Conversely, when intracellular concentrations of thymosin are increased either by overexpression (Yu *et al.*, 1994) or by microinjection (Sanders *et al.*, 1992) cellular levels of F-actin decrease. Tβ4, a 43-residue polypeptide, is the predominant isoform of the β-thymosin family in most mammalian cells, e.g. in resting platelets and neutrophils concentrations up to 5×10^{-4} M are measured (Pantaloni and Carlier, 1993). Under physiological conditions, Tβ4 binds to monomeric actin with an equilibrium dissociation constant (K_d) of 0.4–0.7 μM for platelet actin and 2–3 μM for muscle actin (Weber *et al.*, 1992). Thus, the affinity of Tβ4 for actin is comparable with actin's own affinity for filament ends. In combination with its high abundance, this allows Tβ4 to form a large intracellular pool of sequestered actin monomers, which is readily consumed or restored even upon small changes in the concentration of free G-actin, induced by the capping and/or severing action of other actin binding proteins (Fechheimer and Zigmond, 1993).

In a qualitative study, Vancompernolle *et al.* (1992) outlined the Tβ4 residues 1–24 as the minimal Tβ4 fragment able to mimic wild-type sequestering activity, at least when added in high concentrations. This study focused on the hexapeptide motif ^{17}LKKTET^{22} which is found in all β-thymosin isoforms and is also very conserved in a number of other actin binding proteins including α-actinin, tropomyosin, villin, dematin and actobindin (Vandekerckhove and Vancompernolle, 1992). In the latter the lysine at the second position of the motif can be chemically cross-linked to actin Glu100 (Vancompernolle *et al.*, 1991). Mutating lysine residues 18 and 19 of the hexapeptide motif in the Tβ4 to glutamic acid strongly impaired binding to G-actin. Additionally the presence of an intact N-terminal sequence (1–16) preceding the motif was postulated to be necessary, although its precise role remained unclear (Vancompernolle *et al.*, 1992), and the identity of the residues participating in actin interaction remained elusive.

Although Tβ4 proved to be largely unfolded in solution, NMR analysis in water and in fluorinated alcohols ascribed a strong α-helical tendency to residues 4–16 and to a lesser extent to residues 30–40. The conserved motif ^{17}LKKTET^{22}, following the N-terminal helix, showed no unique three-dimensional fold (Zarbock *et al.*, 1990; Czisch *et al.*, 1993). Therefore, motif and N-terminal helix can also be defined as two separate structural entities.

To understand better the importance of both entities, and of the N-terminal part in particular, we undertook a mutagenesis study using chemically synthesized full-length Tβ4 variants. Our quantitative data allow us to pinpoint Tβ4 residues critical for actin binding. We show that, in addition to residues in the motif, amino acids in

the N-terminus actively participate in binding. The location of these residues indicates that the N-terminal part needs to adopt an α-helix when binding to actin and we derive a model in which a hydrophobic patch of amino acids on one side of this N-terminal α-helix is essential in the contact. A similar separation between a hydrophobic patch and charged residues in the motif is identified in the villin and dematin headpiece. In addition, we observe a competition for binding to actin between Tβ4 and the villin headpiece peptide (VHPp) containing both these entities. Taken together these data suggest that they have (partly) similar binding sites on actin.

Results

The Tβ4 amino acid segment ^{17}LKKTET^{22}, present in all β-thymosin isoforms, has been implicated in actin monomer binding by the study of variants of the Tβ4 fragment 1–30. Also, substitutions in the preceding N-terminal sequence (residues 1–16) analysed in this truncated Tβ4 strongly reduced the inhibition of the salt-induced actin polymerization (Vancompernolle *et al.*, 1992). Although these data were instrumental for delineating regions important for actin binding, subsequent studies proved that the truncated Tβ4-form used (1–30) had too low an affinity to discriminate quantitatively between mutants made in this fragment. Under polymerizing conditions, we determined a K_d of 274 ± 5 μM for the complex of actin and the truncated Tβ4(1–30), which is >40 times that of wild-type Tβ4 (see below).

To characterize the actin binding site of Tβ4 in more detail and to estimate the contribution of each residue critical for contacting actin, we chemically synthesized mutants of the full-length Tβ4 polypeptide. We compared the activity of two classes of Tβ4 variants, carrying either mutations within the motif (17–22) or in the N-terminal segment (1–16), with that of the chemically synthesized wild-type Tβ4, which has been shown in earlier studies to be as active as its biological counterpart (Sanders *et al.*, 1992). Actin-sequestering activity implies not only binding of Tβ4 to actin monomers but also preventing them from associating with other actin molecules, e.g. at filament ends, either by directly masking the actin–actin binding site(s) and/or by inducing a conformational change in the bound actin. Consequently, there is a possibility that binding of the mutants does not necessarily result in actin-sequestering activity. To understand fully the changed activity of the Tβ4 variants we analysed them in three complementary assays: semi-quantitative data of chemical cross-linking and bandshift experiments in native PAGE gave insight in binding to G-actin, and actin polymerization inhibition studies showed the sequestering activity, which was quantitatively expressed in a K_d value.

Mutations in the motif impair actin binding

The motif ^{17}LKKTET^{22} is conserved throughout the β-thymosin family and the first three residues also occur in other actin-binding proteins. In view of this conservation we analysed the substitution mutants L17A, K18E and K19E for binding to monomeric actin. Consistent with earlier results (Vancompernolle *et al.*, 1992), we found that the lysine residues 18 and 19 are of major importance in the actin interaction. While, at an actin concentration of 12 μM, 15 μM of wild-type Tβ4 renders 50% actin–Tβ4 cross-link (Figure 1A and C; Table I), the highest concentration of K19E (240 μM, i.e. 20-fold molar excess over actin) produced only 30% cross-linked product and even at this high concentration K18E cross-linked only marginally. Changing Leu17 into alanine also resulted in a mutant which does not cross-link efficiently. This strongly affected phenotype was confirmed in bandshift experiments. With K19E, complex was still produced at the highest concentration of this Tβ4-variant, but with the mutants K18E and L17A no complex formation could be detected (concentrations of Tβ4 >240 μM resulted in distortions in the electrophoresis pattern and could not be used).

Figure 2 shows the capacity of these mutants to inhibit actin polymerization. Table II gives the derived K_d values. In our assay the wild-type Tβ4 polypeptide has a K_d for binding to monomeric skeletal muscle actin of 6.4 ± 1.6 μM under polymerizing conditions, which is slightly higher than values found in earlier studies (Weber *et al.*, 1992; Pantaloni and Carlier, 1993). All subsequent K_d values listed should be compared with this K_d. Mutant K19E showed a ± 12-fold reduced affinity and, as expected, K18E was more strongly affected, although it still inhibited actin polymerization with a ± 33-fold lower activity than wild-type. Exchanging both Lys18 and Lys19 (KK18,19EE) resulted in total loss of inhibition. The Tβ4 variant in which Leu17 was replaced by Ala was also almost completely inactive. Its affinity for actin was too small to detect any sequestering activity. Taken together, these results indicate that the first three residues Leu17, Lys18 and Lys19 of the conserved Tβ4 motif make specific contacts with actin and/or are necessary for maintaining a correct binding surface. The importance of Lys18 in the actin interaction was further analysed. Compared with K18E, the substitution mutant K18A showed a much less affected phenotype. Binding to G-actin was decreased only 3-fold relative to wild-type (Table I). With a K_d of 75 μM, K18A bound at least 3-fold stronger to monomeric actin in polymerizing buffer than K18E. Taken together, this strongly suggests that Tβ4 Lys18 makes an electrostatic contact with a negatively charged residue in actin and replacing Lys18 by glutamate results in a strong repulsive effect.

Hydrophobic and charged amino acids in the N-terminal segment contribute to actin binding

Like intact Tβ4, the N-terminal segment 1–16 is highly charged (seven of 16 residues) and most charged residues are conserved throughout the β-thymosin family. A number of Tβ4 variants carrying charge reversal substitutions (E/K, D/K and K/E) were synthesized and analysed in the same three assays outlined above (Figures 1 and 2; Tables I and II). In contrast to the mutants studied in the motif which were all affected in their binding capacity, the synthesized mutants in the N-terminus displayed significant differences in cross-linking activity. The K3E, E8K, E10K, K11E and D13K mutants behaved nearly similar to wild-type, indicating that these residues are not involved in actin binding or electrostatic interactions. Surprisingly, substituting Glu8 or Glu10 for lysine even slightly enhanced binding. The only mutants having an unfavourable effect on actin binding were K16E which had a 12-

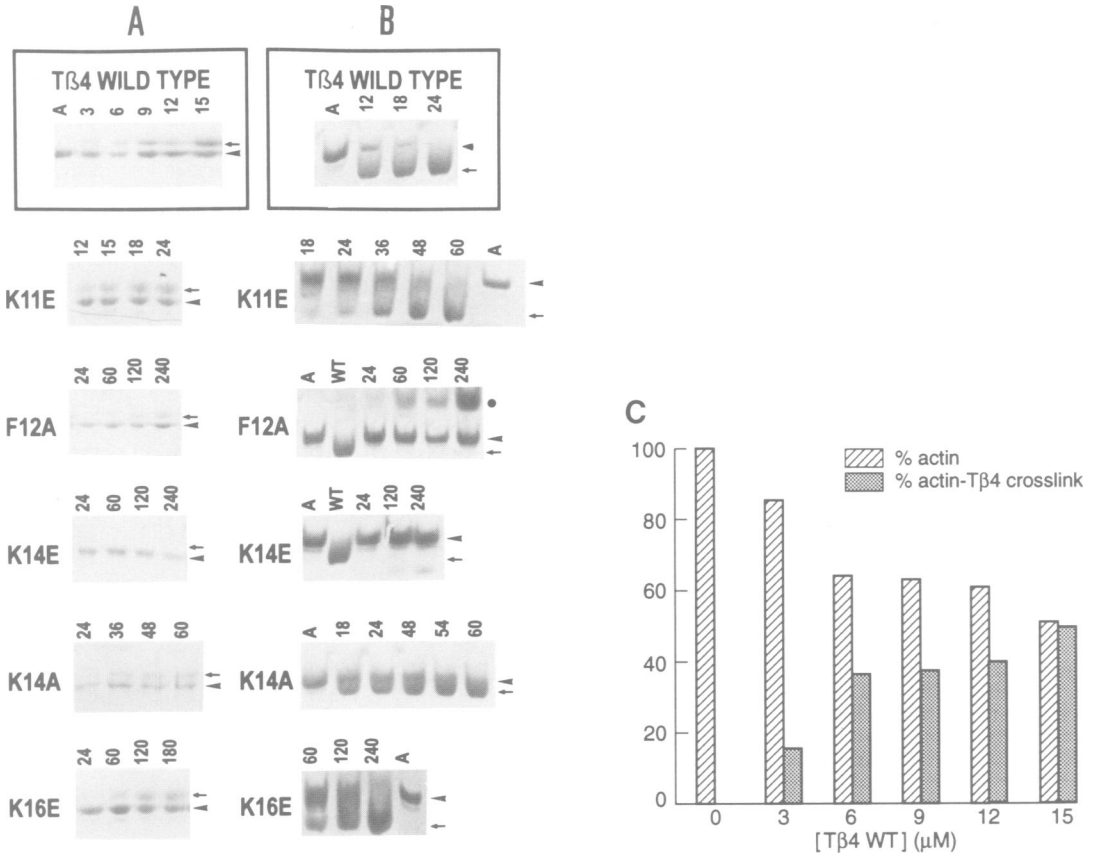

Fig. 1. Binding of Tβ4 wild-type (WT) and Tβ4 variants to monomeric actin through EDC-cross-linking (**A**) and actin–Tβ4 complex formation analysed by non-denaturing PAGE (**B**). (A) G-actin (12 μM), incubated with increasing concentrations of WT or mutant Tβ4 and cross-linker was analysed by SDS–PAGE (12.5%). The micromolar concentrations of Tβ4 are indicated above each lane, the lane headed 'A' shows actin with cross-linker added in the absence of thymosin. The position of the cross-linked actin–Tβ4 complex is indicated by an arrow, the non-cross-linked actin by an arrowhead. All mutants presented in Table I were analysed but only a few representative examples are shown. (B) Mixtures of monomeric actin (12 μM) and various concentrations of Tβ4 (WT or variants) are incubated at room temperature and loaded on non-denaturing polyacrylamide gels (Safer, 1989). The micromolar concentrations of Tβ4 are indicated above each lane. Lanes headed 'A' show actin in the absence of thymosin, while 'WT' represents a sample of 12 μM actin and 24 μM WT Tβ4. Arrows, arrowheads and filled circle indicate the positions of the actin–Tβ4 complex, the non-complexed actin and the free Tβ4 (WT or variant), respectively. Due to charge differences introduced in the Tβ4 variants, the complexes do not all have exactly the same mobility on the native gels. All mutants presented in Table I were analysed but only a few representative examples are shown. (**C**) The molar concentration of Tβ4 (WT or variant) producing 50% cross-link was used as a criterion to determine semi-quantitatively the relative G-actin binding activities. The % actin and % actin–Tβ4 cross-link were determined using densitometric scanning as shown here for WT Tβ4.

fold reduction in relative activity, and K14E which hardly cross-linked to actin monomers, even at the highest concentration used (240 μM). These results were paralleled by the relative activities derived from bandshift experiments (Figure 1B; Table I). In the inhibition assay, E10K, K11E and D13K showed no or only a slight reduction in sequestering activity under polymerizing conditions. The mutants E8K and K3E however (which behaved like wild-type in binding to G-actin in low salt buffer) were more affected in their sequestering activity, resulting in K_d-values of 50 and 94 μM, respectively. K16E had a K_d of 89 μM and for the K14E mutant no or very little sequestering activity was detected under the conditions used, which implies that the K_d must be >1 mM. The role of Lys14 in the actin interaction was further analysed with the substitution mutant K14A. Cross-linking to G-actin was decreased only 4-fold relative to wild-type (Figure 1A; Table I). Moreover, inhibition experiments showed that this substitution has a milder effect than exchanging lysine with glutamate at this position, suggesting that Tβ4 Lys14 makes an electrostatic contact with a negatively charged residue in actin.

As only two charged residues appeared really important and as many protein–protein contacts also depend on hydrophobic and van der Waals interactions, we analysed the significance of the non-polar residues Ile9, Phe12 and of Ser15 in a second series of synthesized variants (Figure 1; Tables I and II). Binding to G-actin in low salt buffer as well as inhibition of actin polymerization in high salt are severely affected by introducing the positively charged lysine instead of Ile9 in Tβ4. Also, replacing the bulky phenylalanine at position 12 by the small residue alanine drastically reduced Tβ4's activity in both low and high salt buffer. Table II shows that conservative F/W and F/Y exchanges are of a much higher tolerance. Comparing the obtained K_d values of 54 μM, 143 μM and ≥1 mM for F12Y, F12W and F12A respectively, suggests that the bulky side-chain of phenylalanine is of major importance

Table I. Semi-quantitative analysis of Tβ4 (wild-type or variant) binding to monomeric actin in low salt buffer

	Cross-linking to monomeric actin[a]			Actin–Tβ4 formation in native PAGE[b]		
	Concentration (μM)	Cross-link formed at this concentration (%)[e]	Relative binding activity	Concentration (μM)	Complex formed at this concentration (%)[e]	Relative binding activity
Tβ4 Wild-type	**15**	**50**	**100**	**24**	**100**	**100**
L17A	240	35	<6	240	–	<<10
K18E	240	15	<6	240	–	<<10
K18A	120	50	12.5	80	100	33
K19E	240	28	<6	240	20	<10
KK18,19EE	240	–[c]	<<6	240	–	<<10
K3E	15	50	100	60	100	40
E8K	12	50	125	[d]		
I9K	240	40	<6	240	–	<<10
E10K	9	50	166	18	100	125
K11E	24	50	62.5	60	100	40
F12Y	30	50	50	30	100	80
F12W	60	50	25	[d]		
F12A	240	25	<6	240	–	<<10
D13K	36	50	42	[d]		
K14E	240	–	<<6	240	–	<<10
K14A	60	50	25	60	100	40
S15A	240	30	<6	240	–	<<10
K16E	180	50	8	240	100	10
del 1–4	42	50	36	60	100	40
del 1–7	240	35	<6	240	–	<<10
K11P	240	10	<6	240	–	<<10

[a]Data derived from experiments as for instance shown in Figure 1A.
[b]Data derived from experiments as for instance shown in Figure 1B.
[c]'–' indicates that no cross-link or actin–Tβ4 complex could be detected at the indicated concentration of Tβ4 variants.
[d]No shift was observed, but competition with wild-type Tβ4 showed they complex actin with an affinity comparable with wild-type.
[e]For the criterion used to express the relative activity of Tβ4 variants see Materials and methods.

Table II. Dissociation constants for binding to monomeric actin under polymerizing conditions

	K_d (μM)		K_d (μM)
Tβ4 wild-type	6.4 ± 1.6	F12Y	54
		F12W	143
L17A	n.s.[a]	F12A	n.s.
K18E	210	D13K	42
K18A	75	K14E	n.s.
K19E	76	K14A	143
KK18,19EE	n.s.	S15A	9
		K16E	89
K3E	95		
E8K	50	K11P	n.s.
I9K	n.s.	del 1–4	103
E10K	2	del 1–7	n.s.
K11E	40		

[a]n.s. (no sequestering) indicates that the Tβ4 variant no longer displays sequestering activity.

in the contact with the actin surface. Substituting Ser15 for alanine had minimal effect on the binding activity, both in low salt and under polymerizing conditions.

Full Tβ4 activity requires an intact N-terminal α-helix

In order to correlate the relative actin binding and sequestering activity of the substitution variants, analysed above, with possible structural changes, especially concerning the integrity of the N-terminal helix, we performed circular dichroism (CD) measurements (Figure 3). CD spectra were recorded not only in H_2O, but also in 60% (v/v) trifluoroethanol (TFE). In aqueous solution (no TFE added) helical characteristics are much less pronounced but the spectra of wild-type and Tβ4 variants relate in the same way as in 60% TFE, which, as reported (Zarbock *et al.*, 1990), stabilizes the helical conformations in the Tβ4 regions of residues 4–16 and 30–40. Thus, in 60% TFE, the increased helical fraction of the conformational population renders the wild-type spectrum the characteristic maximum at 190 nm and the double minima at 207 and 222 nm (Johnson, 1988) (Figure 3A). As Tβ4 has no unique fold in solution, but interconverts between a large number of conformations, these CD data reflect the weighted average of all these states. For this reason the data obtained for the variants were only compared qualitatively with those of wild-type Tβ4. For most mutants described above, we saw only small deviations from the wild-type spectrum, even for the mutants KK18,19EE, K18E and K14E, which had strongly affected phenotypes (Figure 3A and data not shown). Their loss in activity is thus not caused by the fact that they are, on average, no longer capable of forming secondary structures similar to the wild-type protein. The exception is mutant L17A, which displayed a significant increase in helicity, as supported by the more pronounced positive peak at 190 nm and negative peaks at 207 and 222 nm, suggesting that either the N-terminal α-helix is more stable or, more likely, extends over more residues (Figure 3A).

As a control we chemically synthesized a Tβ4 mutant, in which Lys11 was substituted by a proline residue (K11P) and by doing this put a known helix-breaker in the middle of the N-terminal helix. Binding and chemical

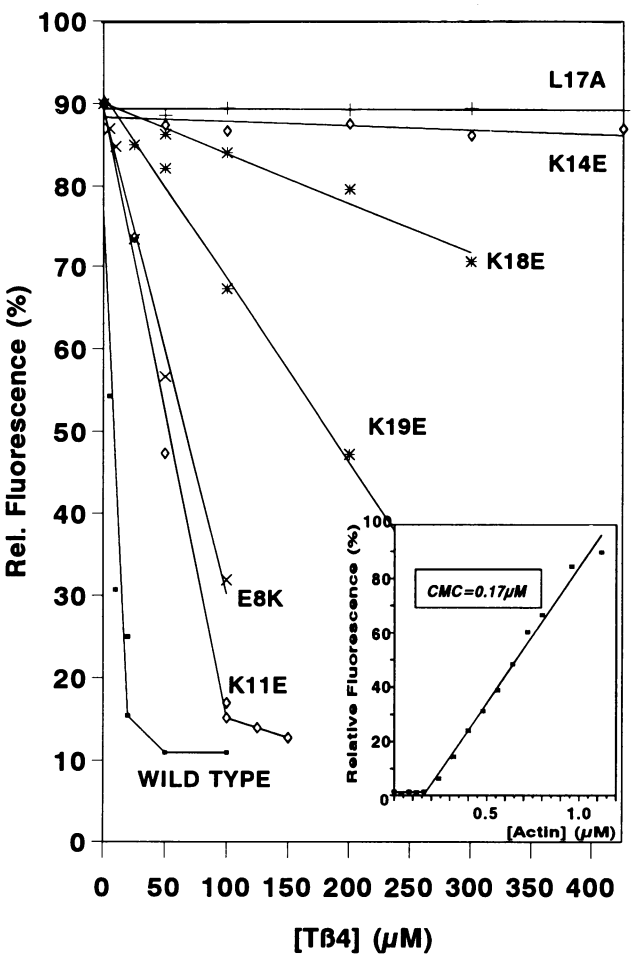

Fig. 2. Polymerization inhibition assay. The steady-state relative fluorescence of samples containing 1 μM F-actin and increasing concentrations of Tβ4 under polymerizing conditions is shown for WT Tβ4 and a few Tβ4 mutants. A representative experiment is shown here; the derived K_d values shown in Table II are calculated using at least two independent experiments. The inset shows the determination of the critical concentration for polymerization as derived from the intercept of the curves of steady-state fluorescence of G- and F-actin (10% pyrene-labelled) versus total actin concentration.

cross-linking of K11P were severely affected (Table I), as was sequestering activity (Table II). (Note that the substitution mutant K11E behaved similarly to wild-type.) The CD spectrum of the K11P variant (Figure 3B) proved to contain less α-helix than wild-type Tβ4, as judged by the decreased intensity of the peak at 190 nm which is characteristic for helical conformation. In addition, this maximum and the first minimum (typically at 207 nm for α-helix) shifted to a lower wavelength, indicating a higher contribution of random coil conformation. Although loss of activity is, as shown above, not linked *per se* to a changed conformation, this last mutation suggests that when altering the integrity of the N-terminal α-helix, activity of Tβ4 is also strongly impaired.

As shorter helices are often less stable, we investigated the importance of the N-terminal part of the helix. The deletion-mutant Δ1–4, which lacks only the first residue of the N-terminal α-helix (Pro4), already had a reduced binding affinity and a K_d of 103 μM, probably due to elimination of K3 (see above). However, the Tβ4 mutant truncated up to residue 8 (Δ1–7) displayed a >16-fold lower capability to cross-link to monomeric actin compared with wild-type and had hardly any sequestering activity (Tables I and II). While the CD spectrum of Δ1–4 is wild-type-like, that of Δ1–7 showed a decrease in overall helicity of the conformational population (Figure 3B). The dramatic loss in binding and sequestering of Δ1–7 can thus be ascribed to a destabilization of the N-terminal helix. In addition, deletion of specific contacts may also have occurred (see Discussion). In summary, changes that affect the integrity of the N-terminal helix are reflected in a reduced activity for actin binding and sequestering.

The actin binding peptide from the villin headpiece competes with Tβ4 for binding to actin

Based upon sequence homology (see Discussion), we identified in the villin and dematin headpiece a similar distribution of hydrophobic residues at the same distance from the LKK-containing motif as in Tβ4. The villin peptide spanning these residues has been shown to bind actin and to induce it to adopt a conformation favourable for actin polymerization (Friedrich *et al.*, 1992). We chemically synthesized the villin peptide (residues 805–826) (Figure 6B), which forms the extreme C-terminus of the protein. This peptide can be cross-linked to G-actin using a zero-length cross-linker (Friedrich *et al.*, 1992; Figure 4). When 24 μM of Tβ4 were incubated with G-actin (12 μM), before incubation with the VHPp, increasing concentrations of the latter were able to displace Tβ4 from actin. Figure 4A shows that the Tβ4–actin cross-link gradually disappears and that, at a concentration of 12 μM of the VHPp, the actin–villin peptide cross-link is almost exclusively formed. Conversely, when actin (12 μM) is first incubated with the VHPp (12 μM), increasing concentrations of Tβ4 can diminish the amount of actin–villin peptide cross-link (Figure 4B). In neither of the conditions was the triple conjugate of actin, Tβ4 and the VHPp observed. The high concentrations of Tβ4 necessary to dissociate the VHPp from actin, suggest a higher affinity of the VHPp, although we learned from time-course experiments that the cross-linking efficiency of this peptide is also much higher (data not shown). The observed competition may be due to two mechanisms. First, binding of the peptides at completely different sites may result in an allosteric change in actin, excluding the binding of the other. However, the pattern of sequence conservation rather suggests another mechanism in which Tβ4 and the villin headpiece bind to overlapping sites in actin.

Discussion

Our binding data allow classification of the analysed Tβ4 residues into three groups according to increasing importance for binding to actin: (i) changes in residues Glu10, Lys11, Asp13 and Ser15 result in variants which hardly differ from wild-type Tβ4; (ii) mutating Lys16 and Lys19 has a weak to moderate effect and (iii) residues Ile9, Phe12, Lys14, Leu17 and Lys18 are extremely important (it must be noted that conservative changes of Phe12 fall into the first two classes). Mutants with changes in Lys3 and Glu8 show differential relative activities, depending on assaying for binding to monomers in G-actin

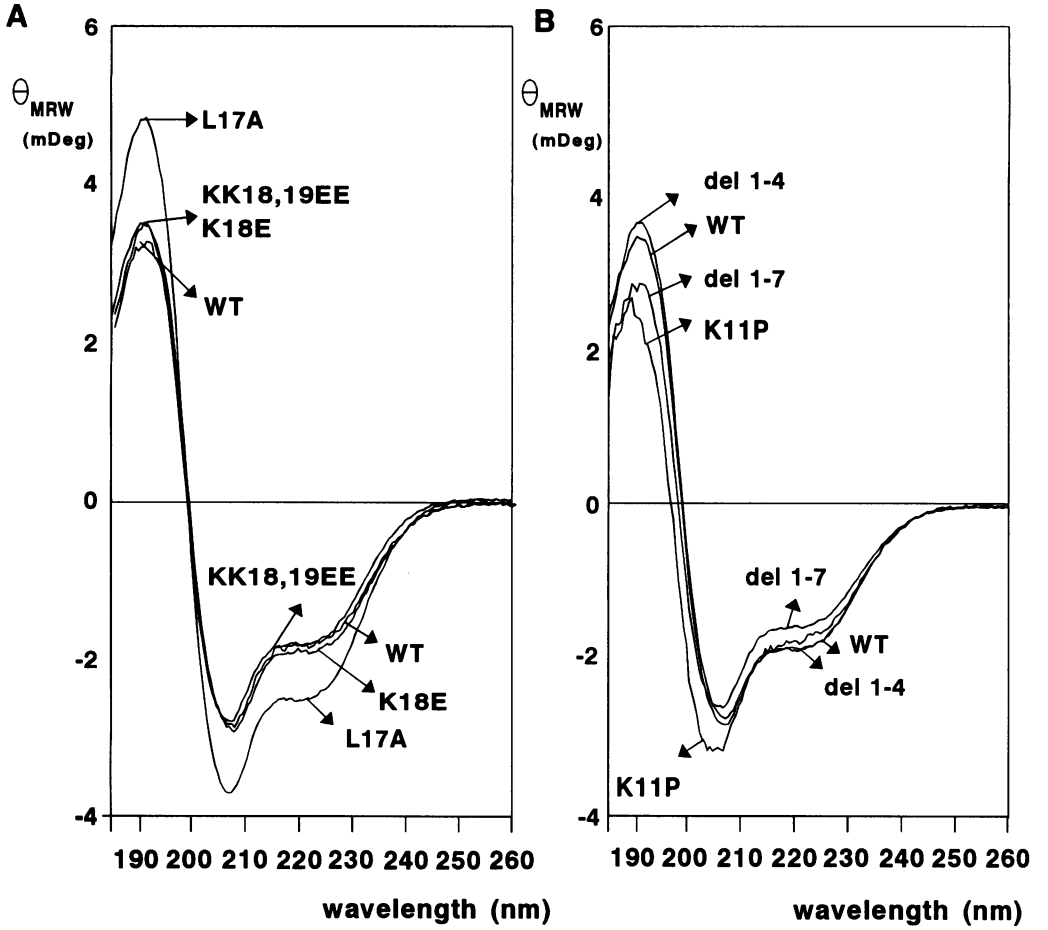

Fig. 3. (**A** and **B**) CD spectra of WT and variant Tβ4 (40 μM) were measured in 60% 2,2,2-TFE. The spectra [mean residue weight elipticity (θ_{MRW}) versus wavelength] are the average of nine scans.

conditions or for inhibition of polymerization and consequent sequestration under polymerizing conditions. These mutants appeared to be relatively more affected in the sequestering assay, which may be due to a lower affinity of these Tβ4 mutants for the changed actin monomer conformation in high salt (Frieden, 1982), or to decreased ability to inhibit actin–actin association, after binding of the Tβ4 variants to monomeric actin with the same affinity as in low salt. One mutant, E10K, slightly improved actin binding; thus, Glu10 must impose some constraint on wild-type Tβ4 activity, possibly by causing a weak repulsion. Alternatively, the E/K exchange might induce a more stable N-terminal helix, e.g. by intrahelical ion-pairing, although our CD data do not support this hypothesis.

We showed that K14 in the N-terminal segment (1–16) and K18 in the conserved motif participate in a specific electrostatic interaction with actin residues. K14A and K18A show a higher binding affinity than K/E substitution mutants, but have no comparable rise in cross-linking yield. This suggests that both lysines are actually cross-linked to a COOH-group of actin upon complex formation. The measured K_d value proved that the K/E exchange at position 14 in the N-terminal segment had a larger effect on Tβ4 activity than a K/E switch at either position 18 or 19, and only introducing the double substitution of residues Lys18 and Lys19 in the motif resulted in a similar decrease in activity.

Both the N-terminal segment (1–16) and the hexapeptide motif (17–22) make interactions (electrostatic and/or hydrophobic) at the actin–Tβ4 interface. We present a model that incorporates these interaction data, defined at the level of primary sequence, in a more structural context. NMR analysis of Tβ4 (Czisch *et al.*, 1993) suggested an α-helix for residues 4–16, a non-defined conformation at residues 17 and 18, a loop structure spanning residues 24–28 and a second, albeit less stable, helical region from residues 30–40. Given these different conformational preferences, the N-terminal helix and the hexapeptide motif ^{17}LKKTET^{22} can be dealt with as separate binding entities. Our binding data strongly support the hypothesis that the N-terminal segment needs to be in a helical conformation for interaction with actin and they allow positioning of a hydrophobic cluster on one side of the N-terminal helix that participates in the actin interaction. It is formed by Met6 (position i), Ile9 (i+3) and Phe12 (i+6) (Figure 5). We include the methionine at position 6 because Jean *et al.* (1994) showed that oxidation of this residue to methionine sulfoxide (thereby introducing a strong dipole) decreased binding affinity of Tβ4 to actin under polymerizing conditions by a factor of 20. Also, we showed that truncation of the N-terminal helix up to residue 8 (Δ1–7, including Met6) resulted in a strongly reduced affinity for monomeric actin in polymerizing buffer. The hydrophilic side of the Tβ4 N-terminal helix is formed by the charged residues Glu8(i+2), Glu10(i+4),

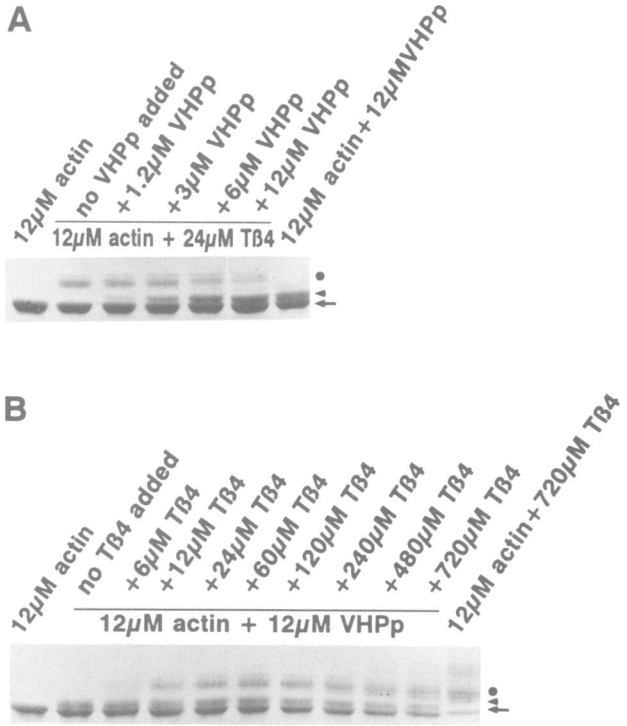

Fig. 4. Competitive binding of Tβ4 and the actin-binding peptide of the villin headpiece. G-actin (12 μM) was incubated consecutively with Tβ4 and VHPp (**A**) or the VHPp and Tβ4 (**B**) before incubation with the cross-linker and analysed by SDS–PAGE (12.5%). The position of actin, the actin–VHPp cross-link and the actin–Tβ4 cross-link are indicated by an arrow, arrowhead and ●, respectively.

Lys11(i+5), Lys14(i+8) and Ser15(i+9) of which only the long side-chain of Lys14 is implicated in a specific contact in the actin–Tβ4 interface.

The importance of the integrity of the N-terminal helix and of the hydrophobic core for the interaction of Tβ4 with actin is further confirmed by the inactivity of the Tβ4 variant K11P. Proline residues do not favour the α-helical configuration (Richardson and Richardson, 1988). The helical content of the K11P mutant is indeed smaller than that of wild-type, as a result of which binding to actin is impaired. We found a similar destabilization of the N-terminal α-helix, resulting in a strongly reduced activity, upon deletion of residues 1–7 (which include part of the hydrophobic cluster, see above).

Similarly, proper termination of the N-terminal α-helix appears important for interaction with actin. This idea is supported by the CD spectrum of the inactive L17A variant, which shows an increase in α-helicity, suggesting that the N-terminal helix in this mutant is longer. In addition, Leu17 in Tβ4 may make a specific interaction, whereby the branched aliphatic side-chain finds its complement in the actin interface.

All residues that proved to be of primordial importance in Tβ4's activity are conserved throughout the β-thymosin family. Only changes ineffective to the chemical nature of the residues have been allowed (Figure 6A). But intriguingly, this conservation can be extended to other actin binding proteins. It was pointed out before that similar hexapeptide motifs exist in a number of actin binding proteins with very diverse actions on actin (Vandekerckhove and Vancompernolle, 1992). Vancompernolle *et al.* (1992) showed that the motif in actobindin formed an actin-binding unit and they proposed a consensus sequence which invariably has leucine at position 1 and basic residues at positions 2 and 3. Substitution of these residues altered actin binding. Also, mutation of the motif in the villin headpiece results, both *in vitro* and *in vivo,* in reduced actin binding (Friedrich *et al.*, 1992).

Here, we show that the actin-contacting site of Tβ4 extends N-terminally from the motif to at least Met6. Using this sequence information, we find that not only the hexapeptide motif, but also the residues forming the hydrophobic cluster in the N-terminal binding site are preserved in other actin binding proteins. We identify a molecular ruler (the same distribution of hydrophobic amino acids at exactly the same distance from the motif) in the actin-binding site of the villin and dematin headpiece domains and there is striking conservation of those residues which we found to be of importance in the Tβ4 N-terminal helix (Figure 6B). This new finding has two important implications. First, the identification of this molecular ruler, suggests that also the distance between both binding entities (the hexapeptide motif on the one hand, and the hydrophobic cluster and charged residue Lys14 on the other) is important to establish contacts in the actin–Tβ4 interface. This hypothesis is supported by data presented above on the inactive L17A mutant, which has an increased α-helicity. If the N-terminal helix is one residue longer, this will result in a considerable shift in the position of the salt bridge forming residue Lys18 and of Lys19 in the motif, a position unfavourable for actin interaction. Additional functional and structural analysis of specifically designed Tβ4 variants probing the relative distance and/or orientation of the two binding entities, will provide insight into the way they relate spatially when binding to actin. Second, the similarity between the actin binding site of Tβ4 and of the villin and dematin headpiece suggests they contact the actin molecule at a similar location. This is strongly supported by the competition we observe between Tβ4 and the VHPp containing the hydrophobic patch and the motif. Conformational changes in actin upon binding of either of the two proteins cannot be ruled out and may contribute to their competitive behaviour. Indeed, subtle differences in the way they bind may be responsible for the opposite effects Tβ4 and the villin headpiece exert on actin polymerization. One example of this may be the fact that the entire actin binding site (including the motif) of the villin headpiece is α-helical (Siminel *et al.*, 1995) and the one of β-thymosin is not (Czisch *et al.*, 1993; this work).

In summary, this report allows a detailed understanding of the actin binding site of the small actin monomer sequestering protein Tβ4 and, awaiting crystallographic data, provides new insights in the way it interacts with monomeric actin. Using functionally complementary assays, which are representative for binding and sequestering activity, we mapped Tβ4 residues of importance in contacting actin. Our data are consistent with a model where the N-terminal segments needs to adopt an α-helical conformation and we identified which side of the α-helix interacts with actin. This information is invaluable for future docking experiments of Tβ4 on the known actin structure (Kabsch *et al.*, 1990).

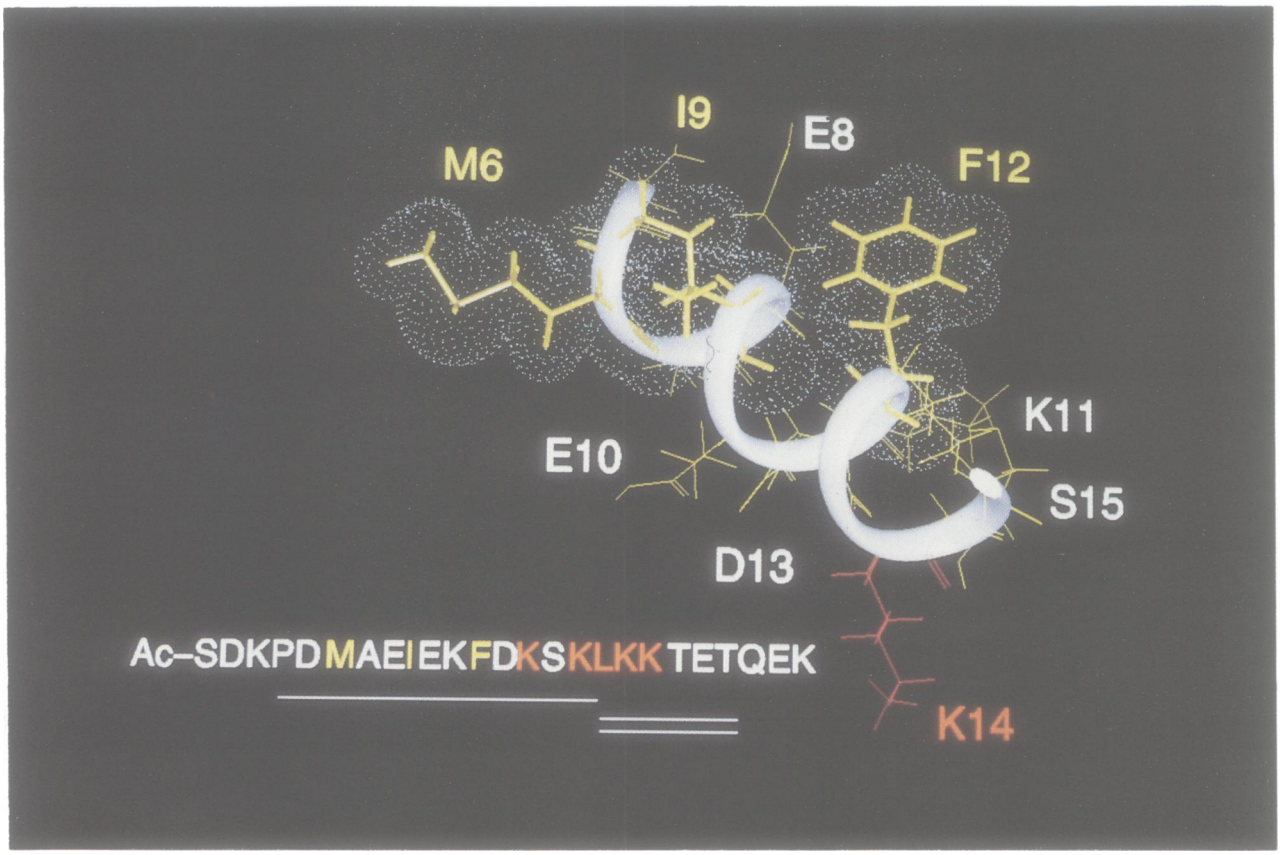

Fig. 5. The N-terminal α-helix (residues 4–16) is shown with the N-terminus in the back of the plane of the paper. The residues Met6, Ile9 and Phe12 (in yellow) forming the hydrophobic cluster on one side of the α-helix, are highlighted and shown with their van der Waals contours. We constructed the α-helical part of Tβ4 with the 'Biosym Builder package' and used the energy minimization algorithm Discover to refine the structure of the peptide (Biosym Technologies, 1994). The position of this α-helix (residues 4–16, underlined) and of the hexapeptide motif (residues 17–22, double underlined) in the minimal actin binding region of Tβ4 (1–25) are shown in the linear sequence at the bottom. Lys14 and the residues in the motif important for interaction with actin are shown in red.

A

```
                  1   5    10   15   20   25   30   35   40
Tβ4          Ac-SDKPDMAEIEKFDKSKLKKTETQEKNPLPSKETIEQEKQAGES-COOH
Tβ4^Ala      Ac-ADKPDMAEIEKFDKSKLKKTETQEKNPLPSKETIEQEKQAGES-COOH
Tβ4^Xen      Ac-SDKPDMAEIEKFDKAKLKKTETQEKNPLPSKETIEQEKQST-COOH
Tβ9          Ac-ADKPDLGEINKFDKAKLKKTETQEKNTLPTKETIEQEKQAK-COOH
Tβ9^Met      Ac-ADKPDMGEINKFDKAKLKKTETQEKNTLPTKETIEQEKQSK-COOH
Tβ10         Ac-ADKPDMGEIAKFDKAKLKKTETQEKNTLPTKETREQEKQEI-COOH
Tβ11_t       Ac-SDKPNLEEVASFDKTKLKKTETQEKNPLPTKETIEQEKQS-COOH
Tβ12_t       Ac-SDKPDLAEVSNFDKTKLKKTETQEKNPLPTKETIEQEKQTA-COOH
Tβ12_p       Ac-SDKPDISEVTSFDKTKLKKTETQEKNPLPSKETAEQEKQAT-COOH
```

B

```
Chicken villin headpiece      805-RSAFANLPLWKQQNLKKEKGLF-COOH
Human villin headpiece        805-PAAFSALPRWKQQNLKKEKGLF-COOH
                                    |   |   |    |||
Thymosin β4                 Ac-SDKPDMAEIEKFDKSKLKKTETQEK-25
                                    |   |   |    |||
Chicken dematin headpiece     362-PEEFGKLALWKRNELKKKASLF-COOH
```

Fig. 6. (**A**) β-Thymosin isoforms. Tβ4 is found in vertebrates together with the less abundant isoforms Tβ9, Tβ10 and $Tβ9^{Met}$. Rabbit and *Xenopus laevis* have a Tβ4-like form: $Tβ4^{Ala}$ and $Tβ4^{Xen}$ respectively. $Tβ11_t$ and $Tβ12_t$ are isolated from trout, $Tβ12_p$ from perch (references in Safer and Nachmias, 1994). Residues of Tβ4 important in actin binding are shown in bold, as are the corresponding residues in the other isoforms.
(**B**) Alignment of the actin binding site of Tβ4, the actin binding part of the villin headpiece domain (Arpin *et al.*, 1988) and the corresponding sequence in the dematin headpiece (Rana *et al.*, 1993). This dematin peptide (362–383) also interacts with actin (J.Gettemans *et al.*, in preparation). Tβ4 residues of the 'hydrophobic cluster' and the motif and the corresponding residues in the other sequences are shown in bold.

Materials and methods

Peptides and proteins

Rabbit skeletal muscle actin was prepared following the procedure of Spudich and Watt (1971) and isolated as Ca–G-actin by chromatography over Sephadex G-200 in G-buffer (5 mM Tris–HCl, pH 7.7, 0.1 mM $CaCl_2$, 0.2 mM ATP, 0.2 mM DTT, 0.01% NaN_3). Actin was labelled with *N*-pyrenyliodoacetamide as described (Kouyama and Michashi, 1981). Tβ4 (residues 1–43), Tβ4 mutants and the VHPp were chemically synthesized on a model 431A peptide synthesizer (Applied Biosystems

Inc., Foster City, CA). Peptides were verified by matrix-assisted laser desorption ionization time of flight mass spectrometry. Purification and concentration measurements of the peptides were performed as in Vancompernolle *et al.* (1992).

G-actin binding assays

Cross-linking experiments. The G-actin solution was dialysed overnight against 5 mM K-phosphate pH 7.5, 0.2 mM $CaCl_2$, 0.2 mM ATP, 0.2 mM DTT. Cross-linking was performed at 12 μM G-actin and various molar ratios of Tβ4 to actin (Figure 1A). After incubation for 20 min at room temperature the zero-length cross-linker, 1-ethyl-3(3-dimethylaminopropyl)carbodiimide (EDC) (Sigma) and *N*-hydroxysulfosuccinimide (Sulfo-NHS) (Pierce) were added to a final concentration of 4 mM (Staros *et al.*, 1986). The reaction was kept at room temperature for another 45 min. Aliquots of the samples were analysed using SDS–PAGE mini slab gels on which the 47 kDa complex can easily be separated from remaining monomeric actin (Figure 1A). At the actin concentration used (12 μM), 15 μM of added wild-type Tβ4 resulted in the formation of 50% cross-linked actin–Tβ4 product (Figure 1C). As a criterion to express the activity of the Tβ4 variants for binding to G-actin relative to wild-type Tβ4, we took the molar concentration of Tβ4 mutants necessary to produce 50% cross-link (see Table I). The % cross-link was measured from two independent experiments via densitometry of Coomassie Blue-stained gels. Representative examples are shown in Figure 1A.

Bandshift using non-denaturing gel electrophoresis. G-actin (12 μM) in G-buffer was mixed with Tβ4 (WT or mutant) at various molar ratios (Figure 1B) and incubated for 20 min at room temperature before adding 0.2 vol of 50% glycerol and loading on native polyacrylamide gels. Gels were prepared according to Safer (1989). The actin–Tβ4 complex ran as a band with a slightly higher mobility than G-actin. Relative binding activities of the mutants are obtained by comparing the concentration necessary to shift all the actin used in the reaction (12 μM) into the complexed form, with that of wild-type Tβ4 producing this same effect (Table I; Figure 1B). When not all the actin was complexed, the % complex formation was obtained using densitometric scanning of Coomassie Blue-stained gels.

Determination of K_d for complexes of actin with Tβ4 or Tβ4 variants

At steady state the amount of F-actin (10% pyrene-labelled) was determined from pyrene fluorescence measurements on a SFM 25 fluorometer (Kontron Instruments, Zurich) using 365 nm as excitation and 388 nm as emission wavelength. Samples containing 1 μM F-actin and increasing amounts of Tβ4 or Tβ4 variants in polymerizing buffer (G-buffer + 100 mM KCl and 1 mM $MgCl_2$) were incubated overnight at room temperature and allowed to reach steady state before measuring. By sequestering actin monomers, Tβ4 reduces the amount of F-actin and consequently the fluorescence signal. This decrease in fluorescence is a measure for the concentration of actin–Tβ4 complex at steady state, as derived from the following.

The equilibrium dissociation constant of the actin–Tβ4 complex

$$K_d = \frac{[A]_{eq}[T]_{eq}}{[TA]_{eq}} = \frac{[A]_{eq}([T]_o - [TA]_{eq})}{[TA]_{eq}} \quad (1)$$

with $[A]_{eq}$, $[T]_{eq}$, $[TA]_{eq}$ equilibrium concentrations of free actin, free Tβ4 and actin–Tβ4 complex; $[T]_o$ is the concentration of Tβ4 initially added. Equation (1) can be written as

$$[TA]_{eq} = \frac{[A]_{eq}}{K_d + [A]_{eq}} [T]_o \quad (2)$$

and is also valid for samples where F-actin, free G-actin, free Tβ4 and Tβ4–actin complex are in equilibrium, which makes $[A]_{eq}$, the concentration of free monomeric actin, identical to the critical monomer concentration (CMC) for actin polymerization. Following the procedure of Pantaloni and Carlier (1993), we determined this CMC in a separate experiment to be 0.17 ± 0.04 μM (see inset and legend for Figure 3). The linear part of this CMC-plot allows us to derive a correlation between the measured fluorescence and the concentration of F-actin expressed as:

$$(\text{Fluorescence} - \text{Fluorescence G-actin}) = 101 \times [\text{F-actin}] + 0.07 \quad (3)$$

Furthermore, the total amount of actin ($[A]_t$) in the absence [eq.(4a)] or presence [eq.(4b)] of Tβ4 can be written as:

$$[A]_t = [FA]_{eq} + [A]_{eq} \quad (4a)$$

$$[A]_t = [FA]_{eq,T} + [A]_{eq} + [TA]_{eq} \quad (4b)$$

with $[FA]_{eq}$ and $[FA]_{eq,T}$ representing steady-state concentrations of polymerized actin in the absence or presence of Tβ4, respectively. As we chose the total actin concentration in our experiments to be constant, equation (4a) equals equation (4b) resulting in:

$$[FA]_{eq} = [FA]_{eq,T} + [TA]_{eq} \quad (5)$$

By introducing equation (2) in equation (5) we get:

$$[FA]_{eq,T} = [FA]_{eq} - [T]_o \frac{[A]_{eq}}{K_d + [A]_{eq}} \quad (6)$$

Thus, from equation (6), the K_d of the complex TA can be derived from the slope $-[A]_{eq}/(K_d + [A]_{eq})$ of the curve $[FA]_{eq,T}$, the steady-state concentration of F-actin in the presence of Tβ4 versus $[T]_o$, or according to equation (3) from the slope of the measured fluorescence versus $[T]_o$ (Figure 2).

Circular dichroism

Far-UV measurements (184–260 nm) were made at room temperature in a JASCO J-710 spectropolarimeter employing a 0.1 mm pathway cell, using a step resolution of 0.5 nm and a scan speed of 20 nm/min. Tβ4 and Tβ4 variants were used in a concentration of 40 μM in 10 mM phosphate buffer, pH 7.4. When added, TFE was 60% (v/v). Differential absorption data for each wavelength are expressed as mean residue weight ellipticity $[\theta_{MRW}]$ (Figure 3).

Competition assay

G-actin [12 μM, in phosphate buffer (see above)] was incubated with a 24 μM of Tβ4 for 20 min at room temperature. The VHPp was added and after another 20 min the cross-linker EDC and Sulfo-NHS were added to a final concentration of 1.5 mM. The cross-linking reaction was kept at room temperature for another 45 min (Figure 6A). The inverse experiment was performed by adding 12 μM of the VHPp to G-actin (12 μM), before incubation with Tβ4 (Figure 6B). Samples in which only Tβ4 or only the VHPp were incubated with G-actin were also included. Aliquots of the samples were analysed by SDS–PAGE.

Acknowledgements

We would like to thank J.-L.Verschelde for preparing the computer image of the Tβ4 helix, J.Van Damme for mass measurements of the synthesized peptides and Prof. M.Rosseneu for use of the spectropolarimeter to perform CD experiments. M.-F.C. would like to acknowledge the Ligne Nationale Française contre le Cancer, the Association pour la Recherche contre le Cancer (ARC) and the Association Française contre le Myopathes (AFM). C.A. is a postdoctoral fellow of the Belgian National Science Foundation (N.F.W.O.). This work was supported by the Human Capital and Mobility Program of the European Community and by EC grant CI1-CT93-0049 and grant 3.0008.94 of the FGWO to C.A. and grant GOA-91/96-3 to J.V.

References

Arpin,M., Pringault,E., Finidori,J., Garcia,A., Jeltsch,J.-M., Vandekerckhove,J. and Louvard,D. (1988) Sequence of human villin: a large duplicated domain homologous with other actin-severing proteins and a unique small carboxy-terminal domain related to villin specificity. *J. Cell Biol.*, **107**, 1759–1766.

Biosym Technologies (1994) INSIGHT II, version 2.3.0. DISCOVER, version 2.9.5. Biosym Technologies, San Diego, CA.

Carlier,M.-F. and Pantaloni,D. (1994) Actin assembly in response to extracellular signals: role of capping proteins, thymosin β4 and profilin. *Semin Cell Biol.*, **5**, 183–191.

Czisch,M., Schleicher,M., Hörger,S., Voelter,W. and Holak,T.A. (1993) Conformation of thymosin β4 in water determined by NMR spectroscopy. *Eur. J. Biochem.*, **218**, 335–344.

Fechheimer,M. and Zigmond,S.H. (1993) Focusing on unpolymerized actin. *J. Cell Biol.*, **123**, 1–5.

Frieden,C. (1982) The Mg^{2+}-induced conformational change in rabbit skeletal muscle G-actin. *J. Biol. Chem.*, **257**, 2882–2886.

Friedrich,E., Vancompernolle,K., Huet,C., Goethals,M., Finidori,J., Vandekerckhove,J. and Louvard,D. (1992) An actin binding site containing a conserved motif of charged amino acid residues is essential for the morphogenic effect of villin. *Cell*, **70**, 81–92.

Jean.C., Rieger,K., Blanchoin,L., Carlier,M.-F. and Pantaloni,D. (1994) Interaction of thymosinβ4 and its variants thymosinβ9 and thymosin β9-met. *J. Muscle Res. Cell Mot.*, **15**, 278–286.

Johnson,W.C. (1988) Secondary structure of proteins through circular dichroism spectroscopy. *Annu. Rev. Biophys. Biophys. Chem.*, **17**, 145–166.

Kabsch,W., Mannherz,H.G., Suck,D., Pai,E.F. and Holmes,K.C. (1990) Atomic structure of the actin:DNaseI complex. *Nature*, **347**, 37–44.

Kouyama,T. and Michashi,K. (1981) Fluorimetry study of N-(1-pyrenyl)iodoacetamide-labeled F-actin. *Eur. J. Biochem.*, **114**, 33–38.

Nachmias,V.T., Cassimeris,L., Golla,R. and Safer,D. (1993) Thymosin β4 in activated platelets. *Eur. J. Cell. Biol.*, **61**, 314–320.

Pantaloni,D. and Carlier,M.-F. (1993) How profilin promotes actin filament assembly in the presence of thymosin β4. *Cell*, **75**, 1007–1014.

Rana,A.P., Ruff,P., Maalouf,G.J., Speicher,D.W. and Chishti,A.H. (1993) Cloning of human erythroid dematin reveals another member of the villin family. *Proc. Natl Acad. Sci. USA*, **90**, 6651–6655.

Richardson,J.S. and Richardson,D.C. (1988) Amino acid preferences for specific locations at the end of helices. *Science*, **240**, 1648–1652.

Safer,D. (1989) An electrophoretic procedure for detecting proteins that bind actin monomers. *Anal. Biochem.*, **178**, 32–37.

Safer,D. and Nachmias,V.T. (1994) Beta-thymosins as actin binding peptides. *BioEssays*, **16**, 473–479.

Sanders,M.C., Goldstein,A.L. and Wang,Y.-L. (1992) Thymosin β4 (Fx peptide) is a potent regulator of actin polymerization in living cells. *Proc. Natl Acad. Sci. USA*, **89**, 4678–4682.

Siminel,C., Rose,T., Goethals,M., Vandekerckhove,J., Friederich,E., Louvard,D. and Delepierre,M. (1995) Conformational behaviour of a synthetic peptide of the C-terminus of villin that interacts with actin: an NMR, CD and simulated annealing study. *Int. J. Peptide Protein Res.*, **45**, 574–586.

Spudich,J.A. and Watt,S. (1971) Regulation of rabbit skeletal muscle contraction. *J. Biol. Chem.*, **246**, 4866–4871.

Staros,J.V., Wright,R.W. and Suringle,D.M. (1986) Enhancement by N-hydroxysulfosuccinimide of water-soluble carbodiimide-mediated coupling reactions. *Anal. Biochem.*, **156**, 220–222.

Vancompernolle,K., Vandekerckhove,J., Bubb,M.R. and Korn,E.D. (1991) The interface of actin and *Acanthamoeba* actobindin. Identification of a new actin binding motif. *J. Biol. Chem.*, **266**, 15427–15431.

Vancompernolle,K., Goethals,M., Huet,C., Louvard,D. and Vandekerckhove,J. (1992) G- to F-actin modulation by a single amino acid substitution in the actin-binding site of actobindin and thymosin β4. *EMBO J.*, **11**, 4739–4746.

Vandekerckhove,J. and Vancompernolle,K. (1992) Structural relationships of actin-binding proteins. *Curr. Opin. Cell Biol.*, **4**, 36–42.

Weber,A., Nachmias,V.T., Pennise,C.R., Pring,M. and Safer,D. (1992) Interaction of thymosin β4 with muscle and platelet actin: implications for actin sequestration in resting platelets. *Biochemistry*, **31**, 6179–6185.

Yu,F.-X., Lin,S.-C., Morrison-Bogorat,M. and Yin,H. (1994) Effects of thymosin β4 and thymosin β10 on actin structures in living cells. *Cell Mot. Cytoskel.*, **27**, 13–25.

Zarbock,J., Oschkindt,H., Hannappel,E., Kalbacher,H. Voelter,W. and Holak,T.A. (1990) Solution conformation of thymosin β4: a nuclear magnetic resonance and simulated annealing study. *Biochemistry*, **29**, 7814–7821.

Received on August 3, 1995; revised on October 4, 1995